10.1071/CH13454_AC

Australian Journal of Chemistry 2014, 67(3), 398–404

Redox Properties of Iron Complexes with Pentadentate Bispidine Ligands

Peter Comba,[A,B] *Hubert Wadepohl,*[A] *and Arkadius Waleska*[A]

[A]Universität Heidelberg, Anorganisch-Chemisches Institut, INF 270, D-69120 Heidelberg, Germany.

[B]Corresponding author. Email: peter.comba@aci.uni-heidelberg.de

Supporting Information

X-ray Crystal Structure Determinations

Crystal data and details of the structure determinations are listed in Table S2. Full shells of intensity data were collected at low temperature with a Bruker AXS Smart 1000 CCD diffractometer (Mo-K_a radiation, sealed tube, graphite monochromator) or a Agilent Technologies Supernova-E CCD diffractometer (Cu-K_a radiation, microfocus tube, multilayer mirror optics). Data were corrected for air and detector absorption, Lorentz and polarization effects; [1-2]**)** absorption by the crystal was treated analytically[2-3], numerically (Gaussian grid)[2, 4] or with a semiempirical multiscan method. [4-6] The structures were solved by the heavy atom method combined with structure expansion by direct methods applied to difference structure factors[7-8] (compound $[(L^4)FeCl_2][FeCl_4]\cdot x\ Bu_2O$) or by the charge flip procedure[9-10] (all others) and refined by full-matrix least squares methods based on F^2 against all unique reflections.[11-13] All non-hydrogen atoms were given anisotropic displacement parameters. Hydrogen atoms were input at calculated positions and refined with a riding model. When found necessary, disordered groups and/or solvent molecules where subjected to suitable geometry and adp restraints. Due to severe disorder and fractional occupancy, electron density attributed to solvent of crystallization was removed from the structures of $[(L^4)FeCl_2][FeCl_4]\cdot x\ Bu_2O$ and $[(NO_2L^4)Fe(MeCN)_2][SO_3CF_3]_2\cdot MeCN\cdot x\ Et_2O$ with the BYPASS procedure,[14] as implemented in PLATON (SQUEEZE).[15-16] Refinement was then carried out against appropriately modified F_{obs}.

CCDC 960718 - 960721 contains the supplementary crystallographic data for this paper. These data can be obtained free of charge from The Cambridge Crystallographic Data Centre via www.ccdc.cam.ac.uk/data_request/cif.

References:

[1] *SAINT,* **1997-2012** (Bruker AXS, Karlsruhe).
[2] *CrysAlisPro,* **2011-2013** (Agilent Technologies UK Ltd., Oxford).
[3] R. C. Clark, J. S. Reid, *Acta Cryst*, **1995**, *A51*, 887.
[4] *G. M. Sheldrick, SADABS-2004-2008 ver. SADABS-2004/1* **2004-2008** (Bruker AXS: Karlsruhe).
[5] R. H. Blessing, *Acta Cryst*, **1995**, *A51*, 33.
[6] *SCALE3 ABSPACK CrysAlisPro,* **2011-2013** (Agilent Technologies UK Ltd., Oxford).
[7] *P. T. Beurskens, G. Beurskens, R. de Gelder, J. M. M. Smits, S. Garcia-Granda, R. O. Gould, DIRDIF-2008* **2008** (DIRDIF-2008, Radboud University Nijmegen, The Netherlands).
[8] P. T. Beurskens, in *Crystallographic Computing 3* (Ed. Sheldrick G.M., Krüger, C., Goddard, R.) **1985**, pp. 216 (Clarendon Press: Oxford, UK).
[9] *L. Palatinus,* **2007** (*SUPERFLIP*, EPF Lausanne: Switzerland).
[10] L. Palatinus, G. Chapuis, *J Appl Cryst*, **2007**, *40*, 786.
[11] *G. M. Sheldrick, SHELXL-97* **1997** (University of Göttingen: Göttingen, Germany).
[12] *G. M. Sheldrick, SHELXL-2012* **2012** (University of Göttingen).
[13] G. M. Sheldrick, *Acta Cryst*, **2008**, *A64*, 112.
[14] P. v. d. Sluis, A. L. Spek, *Acta Cryst*, **1990**, *A46*, 194.
[15] *A. L. Spek, PLATON* **2003** (Utrecht University, The Netherlands).
[16] A. L. Spek, *J Appl Cryst*, **2003**, *36*, 7.
[17] P. Comba, M. Morgen, H. Wadepohl, *Inorg Chem*, **2013**, *52*, 6481.

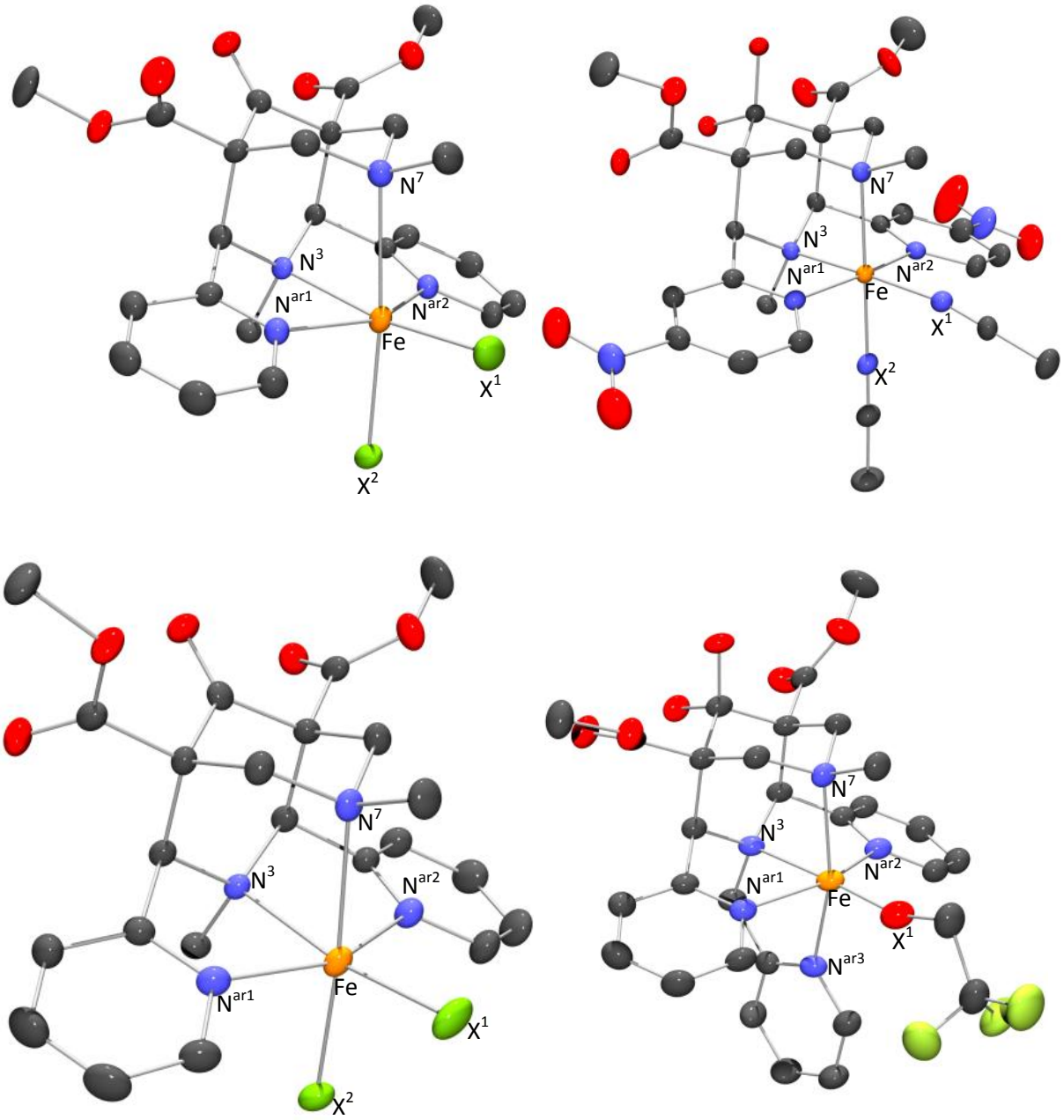

Figure S1. Ferrous compounds top: molecular structure of [(**L**^{4})$FeCl_2$] with C^9 keto function (ellipsoids at 70 % probability) and top right the nitro-substituted [(**NO_2L**^{4})$Fe(MeCN)_2]^{2+}$ with the ketohydrate function (ellipsoids at 50 % probability). Ferric compounds bottom: crystal structure of [(**L**^{4})$FeCl_2]^{+}$ with C^9 keto function (ellipsoids at 70 % probability) and bottom right [(**L**^{3})$Fe(OCH_2CF_3)]^{2+}$ with the ketohydrate function (ellipsoids at 60 % probability). Carbon gray, oxygen red, nitrogen blue, chloride green, iron orange, fluoride pale green, hydrogen atoms omitted for clarity.

Table S1. Selected structural data for the complexes $[(\mathbf{L^4})FeCl_2]$, $[(\mathbf{NO_2L^4})Fe(MeCN)_2]^{2+}$, $[(\mathbf{L^4})FeCl_2]^+$ and $[(\mathbf{L^3})Fe(OCH_2CF_3)]^{2+}$.

Distance/Angle	$[(\mathbf{L^4})FeCl_2]$	$[(\mathbf{NO_2L^4})Fe(MeCN)_2]^{2+}$	$[(\mathbf{L^4})FeCl_2]^+$	$[(\mathbf{L^3})Fe(OCH_2CF_3)]^{2+}$
Fe-N^3	2.2852(18)	1.991(3)	2.2215(16)	2.202(2)
Fe-N^7	2.4857(18)	2.125(3)	2.4057(18)	2.193(2)
Fe-N^{ar1}	2.1481(17)	1.949(3)	2.1057(16)	2.106(2)
Fe-N^{ar2}	2.1407(18)	1.963(3)	2.1183(17)	2.095(2)
Fe-N^{ar3}(X^2)	2.4905(11)	1.941(3)	2.2994(9)	2.093(2)
Fe-X^1	2.3197(10)	1.950(3)	2.2215(16)	1.791(2)
N^{ar1}-N^{ar2}	4.141(3)	3.888(5)	4.109(3)	4.090(3)
N^3-N^7	2.928(3)	2.824(4)	2.923(2)	2.893(3)
∢ (N^3-Fe-N^7)	75.60(6)	86.59(12)	78.25(6)	82.33(7)
∢ (N^{ar1}-Fe-N^{ar2})	149.87(6)	167.49(13)	153.21(6)	153.64(8)
∢ (N^3-Fe-N^{ar3}/X^2)	97.14(4)	92.92(13)	95.40(5)	80.25(8)
∢ (N^7-Fe-X^1)	94.53(5)	95.81(12)	91.89(5)	100.84(8)
∢ (X^1-Fe-N^{ar3}/X^2)	92.76(4)	84.71(13)	94.46(4)	96.59(9)

Table S2. Details for crystal structure determinations.

	$[(L^4)FeCl_2][FeCl_4]\cdot x\ Bu_2O$	$[(L^4)FeCl_2]\cdot 2\ CH_2Cl_2$	$[(NO_2L^4)Fe(MeCN)_2][SO_3CF_3]_2\cdot MeCN\cdot x\ Et_2O$	$[(L^3)Fe(OCH_2CF_3)][SO_3CF_3]_2\cdot MeCN\cdot 3\ CF_3CH_2OH$
formula	$C_{27}H_{35}Cl_6Fe_2N_4O_{5.5}$	$C_{25}H_{30}Cl_6FeN_4O_5$	$C_{35}H_{45}F_6FeN_9O_{17}S_2$	$C_{38}H_{42}F_{18}FeN_5O_{16}S_2$
M_r	827.99	735.08	1097.77	1286.73
crystal system	monoclinic	triclinic	monoclinic	monoclinic
space group	$P\ 2_1/n$	P -1	$P\ 2_1/c$	$P\ 2_1/n$
a /Å	11.273(5)	8.179(4)	16.5278(2)	13.07523(8)
b /Å	11.662(6)	14.681(7)	24.8558(2)	22.83433(12)
c /Å	25.876(13)	14.913(7)	12.1077(2)	17.03336(9)
α /°	90	115.613(7)	90	90
β /°	93.557(8)	104.351(13)	110.9080(17)	102.2596(5)
γ /°	90	95.124(11)	90	90
V /Å^3	3395(3)	1524.2(12)	4646.46(11)	4969.58(2)
Z	4	2	4	4
F_{000}	1692	752	2264	2612

	$[(L^4)FeCl_2][FeCl_4]\cdot x\ Bu_2O$	$[(L^4)FeCl_2]\cdot 2\ CH_2Cl_2$	$[(NO_2L^4)Fe(MeCN)_2][SO_3CF_3]_2\cdot MeCN\cdot x\ Et_2O$	$[(L^3)Fe(OCH_2CF_3)][SO_3CF_3]_2\cdot MeCN\cdot 3\ CF_3CH_2OH$
d_c /Mg·m^{-3}	1.620	1.602	1.569	1.720
X-radiation, λ /Å	Mo-*K*α, 0.71073	Mo-*K*α, 0.71073	Cu-*K*α, 1.5418	Cu-*K*α, 1.5418
μ /mm^{-1}	1.371	1.063	4.376	4.514
max., min. transmission factors	0.9160, 0.6784	0.7464, 0.6729	0.793, 0.530	0.664, 0.344
data collect. temperat. /K	100(2)	100(2)	110.00(10)	115.00(10)
θ range /°	1.58 to 31.00	2.61 to 31.00	3.9051 to 72.0399	3.872 to 72.099
index ranges (indep. set) *h,k,l*	-16 ... 16, 0 ... 16, 0 ... 37 [a]	-11 ... 11, -21 ... 19, 0 ... 21 [a]	-14 ... 12, -30 ... 30, -20 ... 20 [b]	-16 ... 15, -28 ... 28, -20 ... 20 [b]
reflections measured	82905	37651	97815	142336
unique [R_{int}]	10816 [0.0619]	9609 [0.0438]	8994 [0.0701]	9733 [0.0652]
observed [$I \geq 2\sigma(I)$]	8191	7430	8163	9351
parameters refined	365	396	595	729
GooF on F^2	1.015	1.037	1.046	1.040
R indices [$F>4\sigma(F)$] $R(F)$, $wR(F^2)$	0.0369, 0.0786	0.0410, 0.0966	0.0712, 0.1950	0.0498, 0.1372
R indices (all data) $R(F)$, $wR(F^2)$	0.0570, 0.0839	0.0611, 0.1079	0.0770, 0.2002	0.0513, 0.1387
difference density max, min /e·Å^{-3}	0.563, -0.501	0.0746, -0.895	2.762, -1.413	0.953, -0.605

[a] unique set, [b] complete set.

Experimental:

$[(L^4)FeCl_2]\cdot 2\ CH_2Cl_2$ was crystallized by diethylether diffusion into the dissolved ferrous chloride complex (already reported, see main part of this publication for references) in acetonitrile at -20 °C.

$[(NO_2L^4)Fe(MeCN)_2][SO_3CF_3]_2\cdot MeCN\cdot x\ Et_2O$ was crystallized by diethylether diffusion into the solution of 250 mg (0.473 mmol) of ligand[17] and 1 equivalent of ferrous triflate in 5 ml of acetonitrile. No yield was determined due to sole purpose of crystallization.

$[(L^4)FeCl_2][FeCl_4]\cdot x\ Bu_2O$ was crystallized by dibutylether diffusion into a solution of 50.0 mg (0.062 mmol) of the ferrous triflate complex (already reported, see main part of this publication for references) and 1 equivalent of *tris*(4-bromophenyl)aminium hexachloroantimonate in 17 ml of dichloromethane at ambient temperature and inert conditions. No yield was determined due to sole purpose of crystallization.

$[(L^3)Fe(OCH_2CF_3)][SO_3CF_3]_2\cdot MeCN\cdot 3\ CF_3CH_2OH$ was crystallized by diethylether diffusion into a solution of 80 mg (0.086 mmol) of the ferrous triflate complex (already reported, see main part of this publication for references) and 2 equivalents of $^{S}PhIO$ in 10 ml of a mixture of 2,2,2-trifluoroethanol (TFE) / 1,1,1,3,3,3-hexafluoroisopropanol (HFI) 2:1 at -20 °C. No yield was determined due to sole purpose of crystallization.

Table S1. Potentials measured for 1mM **2** in water, containing 0.1 M $NaClO_4$ as supporting electrolyte (Pourbaix Plot, see Figure 4). pH adjusted with $HClO_4$ and NaOH, respectively. P: Species detected at more positive potential, N: species detected at more negative potential.

pH	E_{pa}(P)	E_{pc}(P)	E_{pa}(N)	E_{pc}(N)	$E_{1/2}$(P)	$E_{1/2}$(N)
0.29[a]	0.79	0.689			0.7395	
0.62[a]	0.76	0.674			0.717	
1.08	0.706	0.639			0.6725	
1.52	0.687	0.619			0.653	
1.95	0.67	0.6			0.635	
2.87	0.629	0.551			0.59	
3.56	0.606	0.511			0.5585	
4.21	0.592	0.488			0.54	
5.67	0.584	0.491	0.262[b]	0.186[b]	0.5375	0.224
6.94	0.57	0.465	0.245	0.168	0.5175	0.2065
8.11	0.566	0.47	0.245	0.17	0.518	0.2075
9.34	0.567	0.465	0.247	0.167	0.516	0.207
10.01	0.557	0.465	0.245	0.171	0.511	0.208
10.81	0.53[b]	0.414[b]	0.252	0.167	0.472	0.2095
11.27			0.207	0.134		0.1705
11.69			0.166	0.094		0.13
12.34			0.121	0.0235		0.07225
12.81			0.09	-0.037		0.0265

a: solid compound/not completely dissolved complex

b: no clear assignment possible (saddle points)

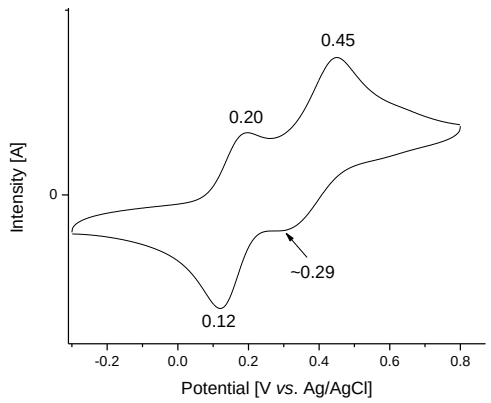

Figure S1. CV of **3** in water with 0.1 M sodium perchlorate as supporting electrolyte and Ag/AgCl reference electrode.

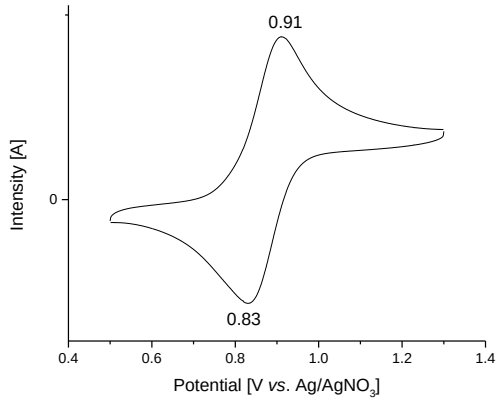

Figure S2. CV of **3** in acetonitrile with 0.1 M TBAHFP as supporting electrolyte and $Ag/AgNO_3$ reference electrode.

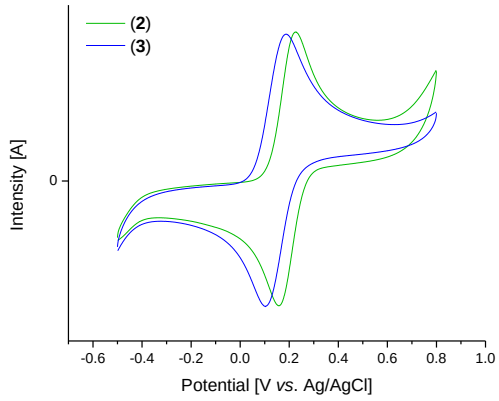

Figure S4. CVs of **2** and **3** in water pH = 11 with 0.1 M sodium perchlorate as supporting electrolyte and Ag/AgCl reference electrode.

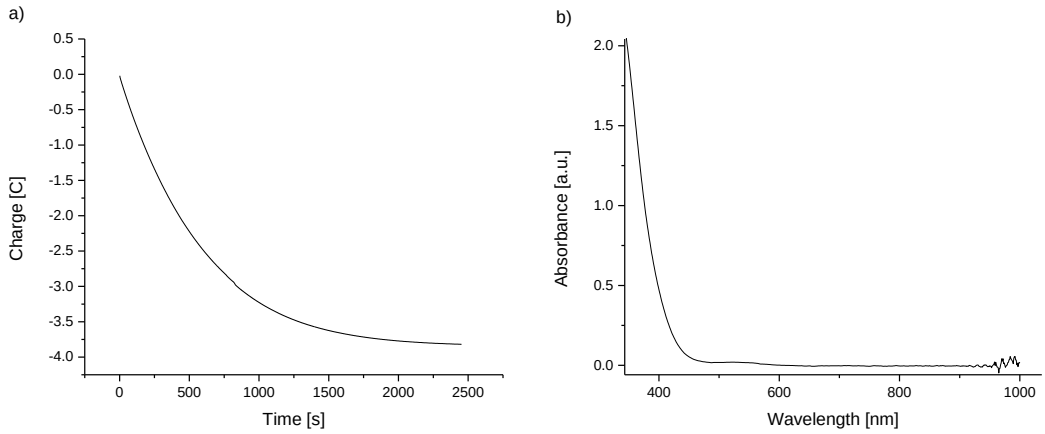

Figure S5. a) Bulk electrolysis (0.8 V *vs*. Ag/AgCl) of 34.1 mg ($38.4 \cdot 10^{-6}$ mol) of **1** in 50 ml 0.1 M NaOAc in water adjusted to pH 4 with HOAc, resulted in the transfer of 3.819 C ≙ $39.6 \cdot 10^{-6}$ mol e^-; 1.031 e^- *per* **1**. b) UV-Vis-NIR spectrum of the 1-e^- oxidized solution.